Linear Arrays with 256 Pixels based on Lithium Tantalate

Reinhard Köhler [1,2], Volkmar Norkus [1,2], Gerald Gerlach [1],
Jens Vollheim [2], Norbert Heß [2], Günter Hofmann [2]

[1] Dresden University of Technology, Institute for Solid State Electronics
[2] DIAS Infrared GmbH

Introduction

Pyroelectric detectors are used as a budget-priced alternative to semiconductor infrared detectors. The application spectrum includes simple motion detectors, non-contact temperature measurement systems, IR spectrometers and gas analyzers, for example.

Based on more than 20 years of experience in development, production and application of pyroelectric single element detectors and detector arrays, a new generation of lithium tantalate linear arrays with better spatial and thermal resolution than in the former detector generation [1, 2, 3] has been developed. Figure 1 shows the fundamental structure of linear pyroelectric arrays.

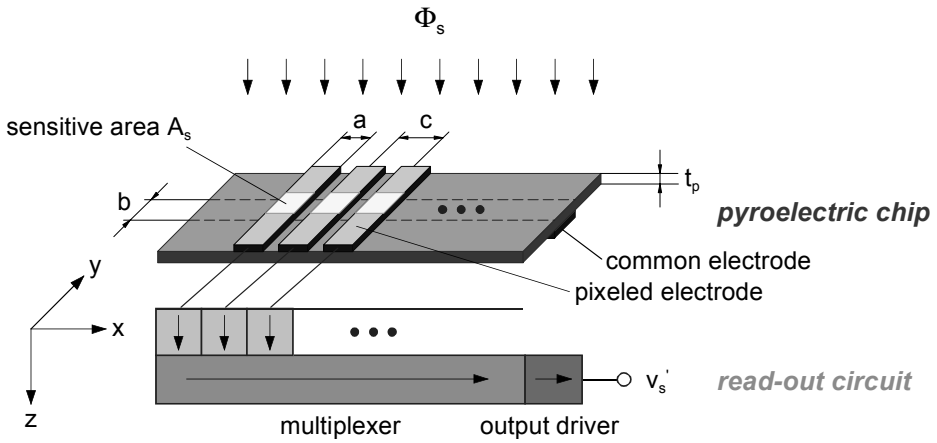

Fig. 1: Fundamental structure of a linear pyroelectric array

In general, $LiTaO_3$ detectors are hybrid components. The introduced linear arrays are an arrangement of a pyroelectric detector chip, printed circuit board (PCB), anisotropically etched silicon aperture and a CMOS read-out circuit in 0.8 µm technique. Interconnections between detector pixels and read-out circuit are carried out by wire bonding. All components are mounted in a hermetically sealed 16 pin metal package. Figure 1 shows a sectional view schematic of the detector array.

Main application are line cameras for temperature measurement in industrial use [4, 5, 8]. One of such cameras, the PYROLINE 256 is shortly characterized in this paper. The PYROLINE 256 cameras provide continuous, non-contact measurement of linear temperature distributions. Operation in conjunction with the IR_LINE software provides data recording, real-time graphical analysis, process integration and camera-control capabilities. The system is based on pyroelectric linear arrays with 256 elements, operating at frame rates of up to 545 Hz. Temperatures between 50 and 1300 °C are measurable in four distinct spectral ranges; 8–14 µm for low temperatures, 3–5 µm for medium temperatures, 4.8–5.2 µm for glass-temperature applications and 1.4–1.8 µm for high temperatures.

1 $LiTaO_3$ Detector Chip Technology

The introduced linear arrays have 256 responsive elements with an area of 40 × 50 µm² arranged in a pitch of 50 µm. Starting material are polarized single-crystal $LiTaO_3$ wafers with a diameter of 2.5″ and a thickness of 500 µm.

First, the wafer is cut into smaller subwafers with an area of about 20 × 20 mm². Afterwards, onto the polished side of the subwafer metallization layers of bottom electrode system ($Ni_{80}Cr_{20}$ and Au) are evaporated and structured by lift-off technique. Difficulties in these steps are caused by the small pattern size (minimum of about 3 µm) in connection with the risk of lightning discharges due to electrification of the pyroelectric material.

In next step, the wafers are fixed onto precision metal plates with less than 5 µm thin special cement. Afterwards, the wafers are thinned down to a thickness of about 40 µm by lapping with silicon carbide, followed by polishing procedure, which reduces the thickness to about 25 µm. After mechanical processing the responsive elements are ion beam etched down to 5 µm. Now the $LiTaO_3$ chip has a 25 µm thick supporting frame and a 5 µm thin area for highly sensitive responsive elements.

The top electrode metallization system is evaporated and lift-off structured again. The responsive elements themselves are coated with low reflecting 10 nm $Ni_{80}Cr_{20}$. An additional gold layer reinforces all other conductive tracks.

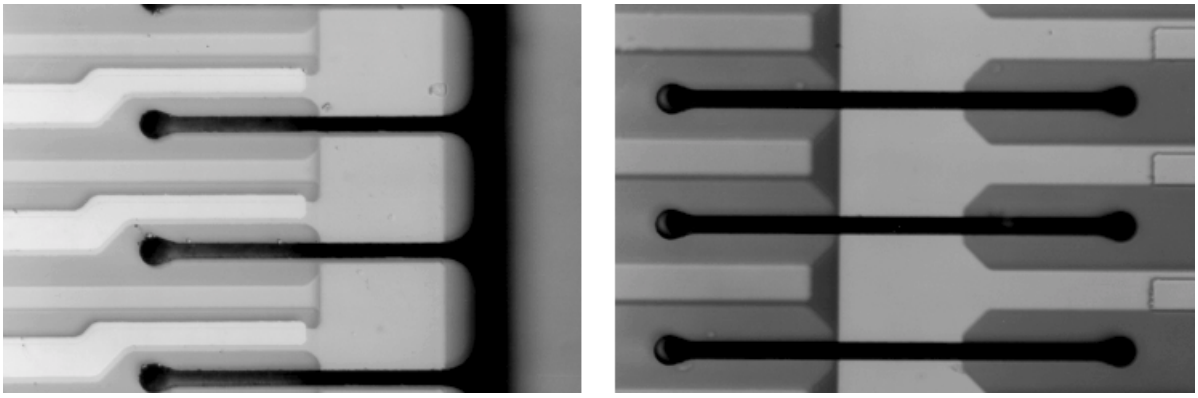

Fig. 2: Detector pixels with ion beam etched trenches (left: reed geometry, right: fence geometry)

In order to minimize the thermal cross-talk small trenches are ion beam etched between the responsive elements. The results of trench etching are two types of thermal insulated pixels – a fence like geometry and a reed like one. Both types are represented in figure 2. In both pictures the pitch of the pixels is 50 µm. The fence like pixel structure is characterized by a higher mechanical stability while the reed structure is better thermally insulated. The applied ion beam etching parameters are strongly dependent on the etching depth, the structure size and the desired side wall angle. Typical parameters and etching rates are shown in table 1.

The etched 5 µm thin $LiTaO_3$ reeds in figure 3 demonstrate the outstanding performance of the ion beam milling process. For etching mask photo resist AZ 4562 has been used.

Table 1: Ion beam etching parameters for $LiTaO_3$

	accelleration voltage V_{acc} in V	ion current density S_I in mA / cm²	$LiTaO_3$ etching rate in µm / h	photo resist etching rate in µm / h
normal power	800	0,6	2.3–2.4	1.55–1.75
low power	250	0,6	1.04–1.27	0.59–0.77

The two ion beam etching processes described above, simultaneously separate the 10 linear array detector chips placed on one subwafer.

Finally, the chips are detached and cleaned. In order to cure damages, which were caused by ion beam etching processes, the chips are annealed by a soft thermal treatment.

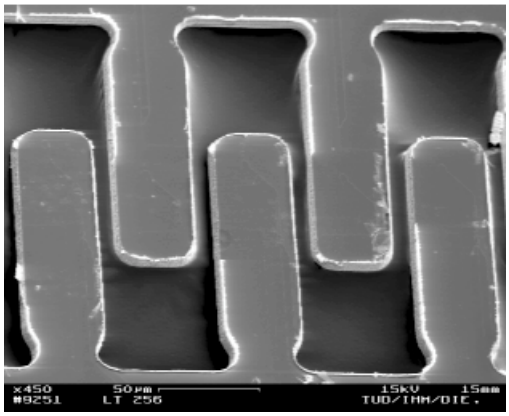

Fig. 3: SEM image of $LiTaO_3$ reeds (50 µm pitch)

2 Read-out Circuit

The 75 mW consuming read-out circuit is especially designed for detectors with 256 pixels. The circuit is produced in 0.8 µm CMOS technology. It consists of an analogue and a digital part and is optimized for low noise and high linearity. Figure 4 shows the circuit diagram of its analogue path. First stage works as a charge-current transducer in which the pyroelectric elements are operated in current mode. After integration each signal is stored in a sample-&-hold stage. Finally, the 256 channels are switched to the output driver by a multiplexer.

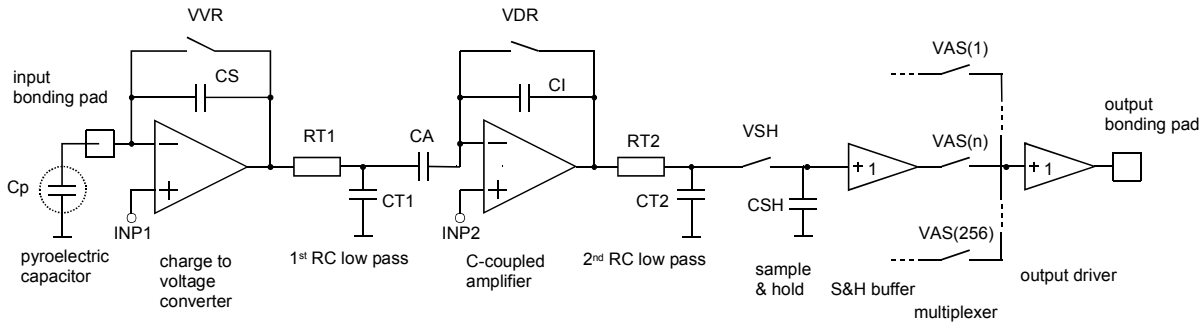

Fig 4: Circuit diagram of analogue path of the read-out circuit

3 Detector Assembly

As mentioned above, the detectors are hybrid arrangements. An adhesive onto a micromachined silicon carrier bonds the fragile $LiTaO_3$ chips. Simultaneously, this carrier acts as an optical aperture, i.e. as an optical shield against heat absorption in the pixel surroundings. Afterwards, both the sandwich construction and the read-out circuit are mounted onto PCB with a conductive adhesive. For the connections between read-out circuit and PCB thermal compression bonding is used whereas the connections between pyroelectric chip and input stages of read-out circuit are realized by ultrasonic fine

pitch bonding. A special bonding wedge is used together with an AlSi wire with a diameter of 17.5 µm in order to produce bonds with a pitch of 50 µm.

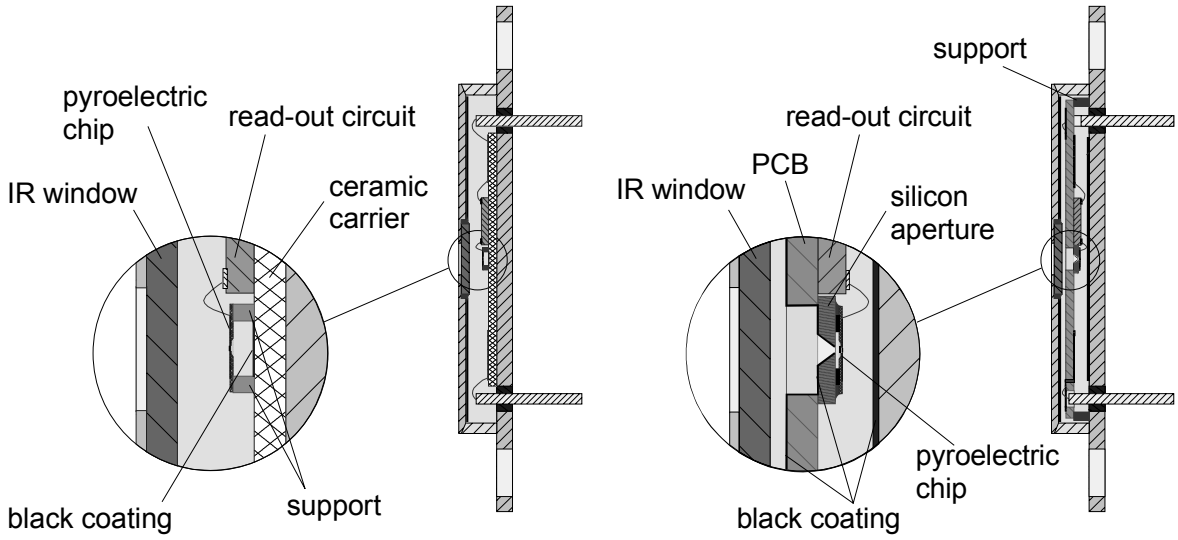

Fig. 5: Sectional view of 256 pixels $LiTaO_3$ linear arrays (left: without silicon aperture and absorption black, right: with silicon aperture and absorption black)

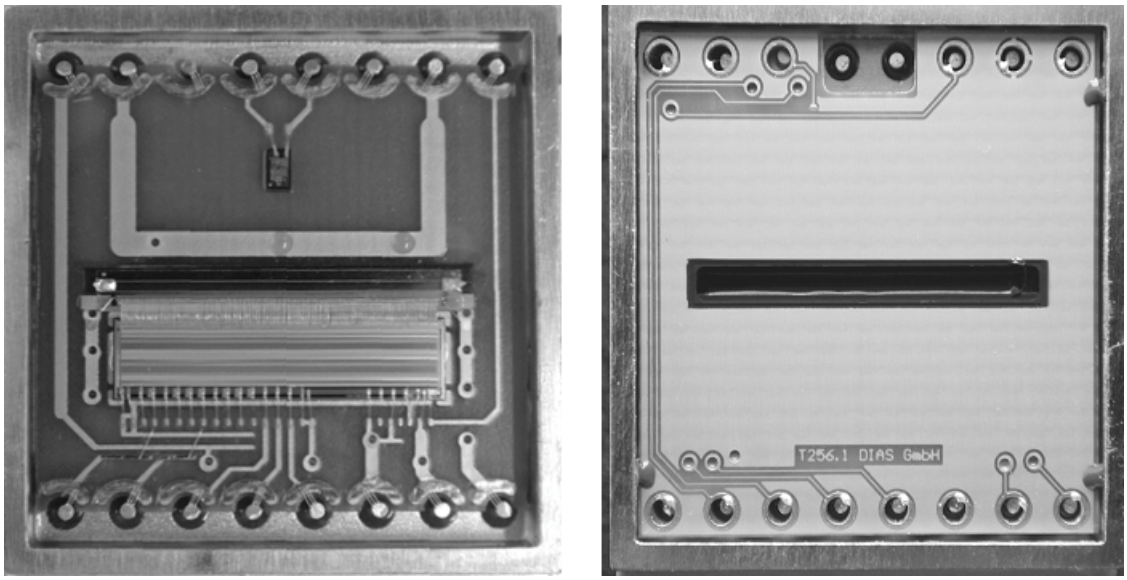

Fig. 6: $LiTaO_3$ arrays in metal package without lid
(left: standard assembly, right: face down assembly)

For optimum heat absorption a broadband absorbing black coating or a special λ/4 thin film absorber can be used. Regardless of the application of an absorber on top of the responsive elements, the silicon precision aperture must be black coated in order to avoid heat radiation transmission and reflexion inside the package. Before this black coating, the PCB with the parts has to be mounted face down into the case header. The connections between PCB and package pins are bonded. An AD590 temperature detector is integrated onto the bottom of the housing as well.

Now the absorber can be deposited. A silver black coating has been optimized for the $LiTaO_3$ detectors. The coating with a thickness of about 5 µm is electrically conductive and is distinguished by a

band absorbance of about 0.92 for a 500 K black radiator in the range of 2–20 µm [6]. Optional with the application, the spectral range can be determined within 1.2 µm and 20 µm by a band pass window in the lid of the package. Finally, the package is sealed hermetically. In addition, a detector type without absorption black and silicon aperture enables a more easy assembling but doesn't have as high performance as the more complicated one. In this case PCB with detector chip is not face down mounted.

In figure 5 both types are represented schematically. Figure 6 shows completely mounted (except the lid) arrays of both 256 pixels arrays.

4 Detector Characteristics

The described detectors are still under development. All detector measurements has been performed in unsealed packages, without black coating and with an antireflection-coated 8–14 µm Ge filter.

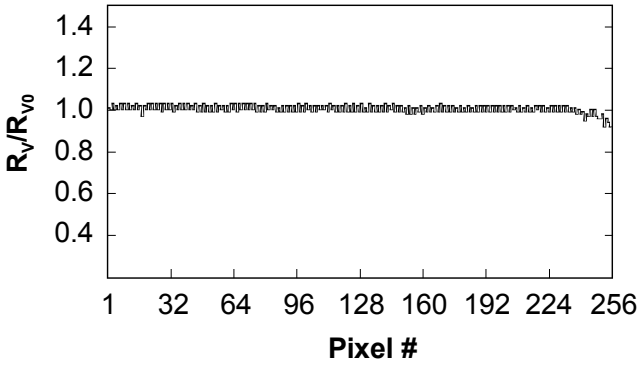

Fig.7: Responsivity distribution of a $LiTaO_3$ array without trenches at f_{mod} = 128 Hz

Its voltage responsivity amounts up to more than 600.000 V/W at a rectangular modulation frequency f_{mod} = 128 Hz. The voltage responsivity distribution R_V / R_{V0} of a detector without trenches at a modulation frequency of 128 Hz is shown in figure 7.

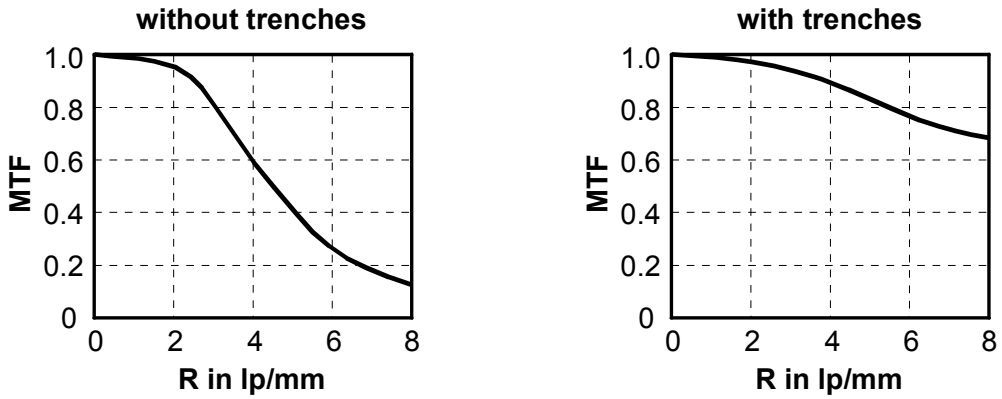

Fig. 8: Measured MTF of two $LiTaO_3$ arrays with 256 pixels at f_{mod} = 128 Hz

Figure 8 shows the improved modulation transfer function MTF of a detector with thermal insulating trenches in comparison to a detector without trenches each at modulation frequency of 128 Hz. As a result of the improved thermal insulation between the responsive elements, the MTF is better than 0.8 at spatial frequencies R up to 5 lp/mm. There is no difference between fence structure and reed structure, neither in MTF nor in NEP.

In table 2 the measured values, desired values of the arrays with 256 pixels and comparative values of current detectors with 128 pixels are listed. The values are from arrays without absorption black. The enhanced MTF of detectors with thermal insulating trenches between the pixels demonstrates the strong influence of this design improvement. The comparison with the current detectors with 128 pixels shows the high performance of the new arrays. Noise equivalent power NEP amounts without software averaging to 1.1 nW at 128 Hz for a detector with trenches and a thickness of the sensitive elements of 4.8 µm. The higher NEP of the detector without trenches is caused by the thicker elements (5.5 µm). All the introduced detectors are optimized for modulation frequencies of 128 Hz or higher.

Table 2: Table of $LiTaO_3$ linear array characteristics

	Desired value	Measured value		Comparative value (128 pixel array)
$LiTaO_3$ chip	with trenches	with trenches	without trenches	
Pixel width	> 40 µm	40 µm	42 µm	90 µm
Pixel length	50 µm	50 µm	50 µm	100 µm
Pitch	50 µm	50 µm	50 µm	100 µm
Element thickness	5 µm	4.8 µm	5.5 µm	20 µm (LT) 5 µm (LT-I)
MTF	0.8 (@ 5 lp/mm)	0.8 (@ 5 lp/mm)	0.4 (@ 5 lp/mm)	0.6 (@ 5 lp/mm)
NEP	1–1.5 nW	1.1 nW	1.4 nW	5 nW (128 LT) 2 nW(128 LT-I)
Inhomogenity of Responsivity	5 %	5.5 %	1,7 %	< 2 % (128 LT) < 5 % (128 LT-I)
Modulation frequency	≥ 128 Hz	128 Hz	128 Hz	128 Hz

5 Camera System

The camera system PYROLINE 256 was developed for use with pyroelectric linear 256-element-arrays 256-LT-I. Fig. 9 shows the complete camera. It consists of a robust, industrial housing that can be equipped with integrated water-cooling and air purge for lens system. The camera includes the pyroelectric array, a chopper module (chopper frequency 545 Hz), the IR-optics as well as the entire analog and digital signal processing.

Fig. 9: Infrared line camera PYROLINE 256

Four basic device variations for different applications were developed. Essential technical data are summarized in Table 3. The standard temperature ranges include temperatures of 50–1300 ºC. Spectral ranges are 8–14 µm for low-temperature applications, 3–5 µm for measurement of medium temperatures, 4.8–5.2 µm for glass applications and 1.4–1.8 µm for high temperature measurements.

Table 3: Selected technical data of the line camera PYROLINE 256

PYROLINE	256	256 M	256 G	256 H
Spectral range	8–14 µm	3–5 µm	4.8–5.2 µm	1.4–1.8 µm
Measurement temperature range[a]	50–550 °C / 450–1250 °C	450–1250 °C	450–1250 °C	600–1300 °C
Aperture	40° x 0.3°	60° x 0.5°	60° x 0.5°	60° x 0.5°
Spatial resolution (50 % modulation)	3 mrad	4 mrad	4 mrad	4 mrad
Measurement distance	10 cm – infinity	20 cm – infinity	20 cm – infinity	50 cm – infinity
Accuracy[b]	2 K up to 100 °C or 1 K + 1 % of true value	1 K + 1 % of true value	1 K + 1 % of true value	1 K + 1 % of true value
Frame rate	internal 544 Hz, selectable 272 Hz, 136 Hz, ...			
Response time	internal 4 ms, selectable: 2/ measurement frequency			
Interface	PCI-PC-card, fiber optic connection			
Connectors[c]	round connector with thread interlocking (16-pins) interlocking fiber optic- connector (2-fibers) water supply tubing (nominal width 4 mm, 2 bar max) compressed air tubing (nominal width 4 mm, 2 bar max)			
Housing	IP65, optional with integrated water cooling system, air purge, swivel base			
Weight	ca. 3.2 kg			
Supply voltage	18–36 V DC / 10–20 VA			
Operating temperature	Camera: 0–50 °C, –25–150 °C (with water cooling) system cable: –25–150 °C fiber optic: 0–70 °C			
Storage condition	–20–70 °C, relative humidity 95 % max			
Software	computer control and display program for Windows™			

[a] different on request,

[b] for black body and ambient temperature 25 °C,

[c] depending on configuration

Figure 10 shows the block diagram of this camera. The signal processing electronics includes:

- Close to sensor electronics
- Digital clock pulse generator
- Analog-to-digital converter
- Image difference processing (IDP)
- Chopper motor controller
- Sensor temperature stabilization
- Printed circuit board for signal input and output
- DC/DC- printed circuit board

Operation of the camera, image acquisition and data processor are controlled using the “IR_LINE” software, which communicates with the camera via a dedicated PCI card and fiber-optic cable.

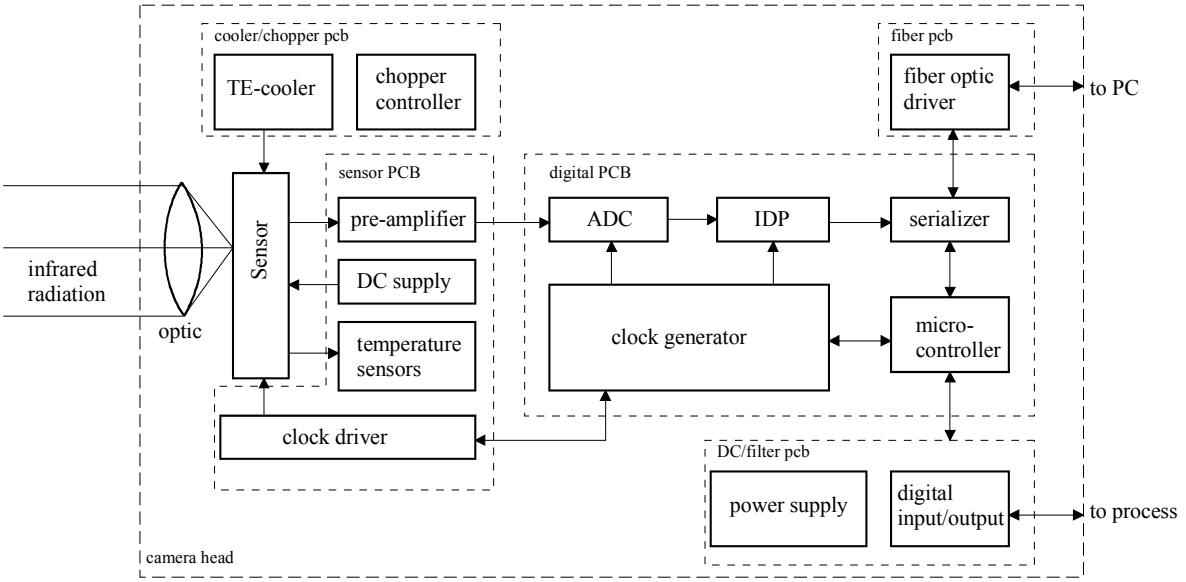

Fig. 10: Block diagram of the camera electronic PYROLINE 256 [8]

6 Acknowledgements

This work was supported by the Federal Ministry of Education, Science, Research and Technology (BMBF) under contracts № 16SV1094/0 and № 16SV1095/2.

References

[1] T. Sokoll, V. Norkus, G. Gerlach, "Thermal and Spatial Resolution of Pyroelectric Linear Arrays", Proc. 3rd THERMINIC workshop, Cannes, pp. 217-222, 1997

[2] V. Norkus, G. Gerlach, G. Hofmann, "Uncooled linear arrays based on $LiTaO_3$", Proc. of 9th Int'l Conference for Sensors, Transducers & Systems, Nürnberg, pp. 23-28, May 18-20, 1999

[3] V. Norkus, G. Gerlach, G. Hofmann, "High-resolution infrared detectors based on $LiTaO_3$", Proc. of 3rd OPTO Conference, Erfurt, pp. 23-28, May 18-20, 1998

[4] V. Norkus, T. Sokoll, G. Gerlach, G. Hofmann, "Pyroelectric infrared arrays and their applications", SPIE Infrared Spaceborne Remote Sensing V, Vol. 3122, pp. 409-419, 1997

[5] F. Nagel, M. Zimmerhackl, "Spectrometer assembly with a pyroelectric array", 5th conference "Infrared Sensors and Systems", Dresden, Dresdner Beiträge zur Sensorik, vol. 4, pp. 113-117, 1997

[6] V. Norkus, G. Gerlach, G. Hofmann, "Process Technologies for High-Resolution Infrared Detetors based on $LiTaO_3$", Device and Process Technologies for MEMS and Microelectronics, Proc. of SPIE, vol. 3892, Brisbane, pp. 233-240, 1999

[7] V. Norkus, G. Gerlach, and G. Hofmann, "High-resolution pyroelectric linear arrays based on $LiTaO_3$", SPIE 4369, pp. 322-331, 2001

[8] P. Drögmöller, G. Hofmann, H. Budzier, Th. Reichardt, M. Zimmerhackl, "Infrared line cameras based on linear arrays for industrial temperature measurement", to be published in SPIE Thermosense, Orlando, April 2002